JOURNAL OF MATERIALS SCIENCE: MATERIALS IN MEDICINE 4 (1993) 266–272

Particulate dental composites under sliding wear conditions

K. FRIEDRICH
Institute for Composite Materials Ltd, University of Kaiserslautern, 6750 Kaiserslautern, Germany

The wear of behaviour of dental composites, consisting of glass particles in a PMMA-matrix, is investigated under dry sliding conditions against a smooth hardened steel surface. Wear mechanisms were identified, such as plowing and patch formation; their individual contribution to the total wear of the composite is a function of particle size, filler content and filler/matrix adhesion. In addition, the inter-particle-distance determines the transition from one dominating mechanism to the other.

1. Introduction

Reinforcement of polymers by high-modulus fibres results in composite materials of high modulus with tensile strength and toughness which can be greater than those of the component materials. Hard-particle reinforcement of glassy or crystalline polymers gives an increase in modulus but no improvement or a reduction in tensile strength and impact strength. Particle-filled polymer composites are thus suited to uses where a high modulus is needed, where loads are mainly compressive or where high-temperature creep resistance is important.

Dental filling materials are one such application. The requirements for a suitable material are that it can be inserted into a cavity as a viscous liquid or paste and will rapidly set. It should provide a good match to natural tooth in modulus, thermal diffusivity and thermal expansion. Also the material should be wear resistant and dimensionally stable so that it fits tightly into the cavity without leakage. Amalgam is generally used to fill cavities in the occlusal (grinding) surfaces of posterior molar teeth but has the disadvantage of being unaesthetic in front teeth. Silicate cements are used for filling front teeth but these have poor mechanical properties and slowly dissolve so that the filling lifetime varies between 1 and 10 years but typically is only about 5 years. In the 1950s polymeric filling materials were tried but were unsatisfactory as they wore rapidly, showed excessive polymerization shrinkage and had a coefficient of thermal expansion which was much greater than that of teeth [1]. Subsequently, particle-filled polymer composites were developed with much improved properties.

The main problems with dental composite resins, as deduced from an analysis of the reasons given for replacement, are insufficient wear resistance; insufficient marginal integrity or sealing ability, which is suspected to lead to secondary caries formation; and to a lesser extent insufficient colour stability. *In vivo* studies have shown that surface erosion and abrasion occurs in the contact-free areas as well as in the occlusal-contact areas of posterior composites. There are several methods available to analyse wear and abrasion resistance *in vitro*, including: two-body abrasion, three-body abrasion, oscillatory wear and chewing simulation. A three-body abrasion apparatus capable of varied sliding action at the interface has produced good correlation with *in vivo* data [2, 3]. The results of these studies were dependent upon the choice of third-body abrasive and the mechanical settings employed for speed and load. This method for evaluating wear resistance of posterior composites shows promise as a predictive tool for different types of composites. However, results are presently inconclusive due to the complexity of the wear process in the oral cavity.

The purpose of the present study was to investigate how this group of materials performs under wear conditions against a smooth metallic counterpart. In particular, it should be demonstrated how various material compositions (with regard to variations in particle size and their bonding to the surrounding polymer matrix) influence the wear rate of the material, and which mechanisms dominate the wear processes.

2. Material compositions

For the dental composite in this study, a polymethylmethacrylate (PMMA) based matrix (special composition DPMA/TEGDM = 67/33) was filled with different amounts of glass (Gd 83-type) particles. Two monomodal sizes of $d = 2$ and slightly less than 10 μm, respectively, were used [4]. A further subdivision is that groups with and without silane coupling agent on the filler were tested. Table I shows the formulation details, i.e. composite identification code, nominal and actual filler volume fraction (as determined from density measurements with $\rho_{Filler} = 3.2\ g\,cm^{-3}$ and $\rho_{Matrix} = 1.18\ g\,cm^{-3}$), filler particle size and type of surface treatment. Cross-sections of specimens having different amounts and sizes of the

0957–4530

TABLE I List of nominal and actual filler volume fractions in the different dental materials used for the sliding wear studies

Material code	Filler particle size d (μm)	Nominal volume fraction V_f (%)	Actual volume fraction V_f (%)	Surface treatment	Symbols
55	—	—	—	Matrix	□
60A	< 10	60	58.6	No silane	
60B	< 10	50	47.9	No silane	
60C	< 10	40	35.2	No silane	◇
60D	< 10	30	25.4	No silane	
60E	< 10	20	16.1	No silane	
60F	< 10	10	5.3	No silane	
62A	< 10	60	59.1	With silane	
62B	< 10	50	49.4	With silane	
62C	< 10	40	38.4	With silane	○
62D	< 10	30	27.9	With silane	
62E	< 10	20	18.5	With silane	
62F	< 10	10	7.7	With silane	
64A	2	55	55.3	No silane	
64B	2	50	47.8	No silane	
64C	2	40	39.6	No silane	△
64D	2	30	27.3	No silane	
64E	2	20	13.8	No silane	
64F	2	10	3.4	No silane	
66A	2	55	55.3	With silane	
66B	2	50	49.9	With silane	
66C	2	40	39.6	With silane	▽
66D	2	30	30.6	With silane	
66E	2	20	18.0	With silane	
66F	2	10	9.2	With silane	
68A	2	55	53.6	With silane[a]	
68B	2	20	17.8	With silane[a]	▼

[a] plus antioxidant (Trigonox 21)

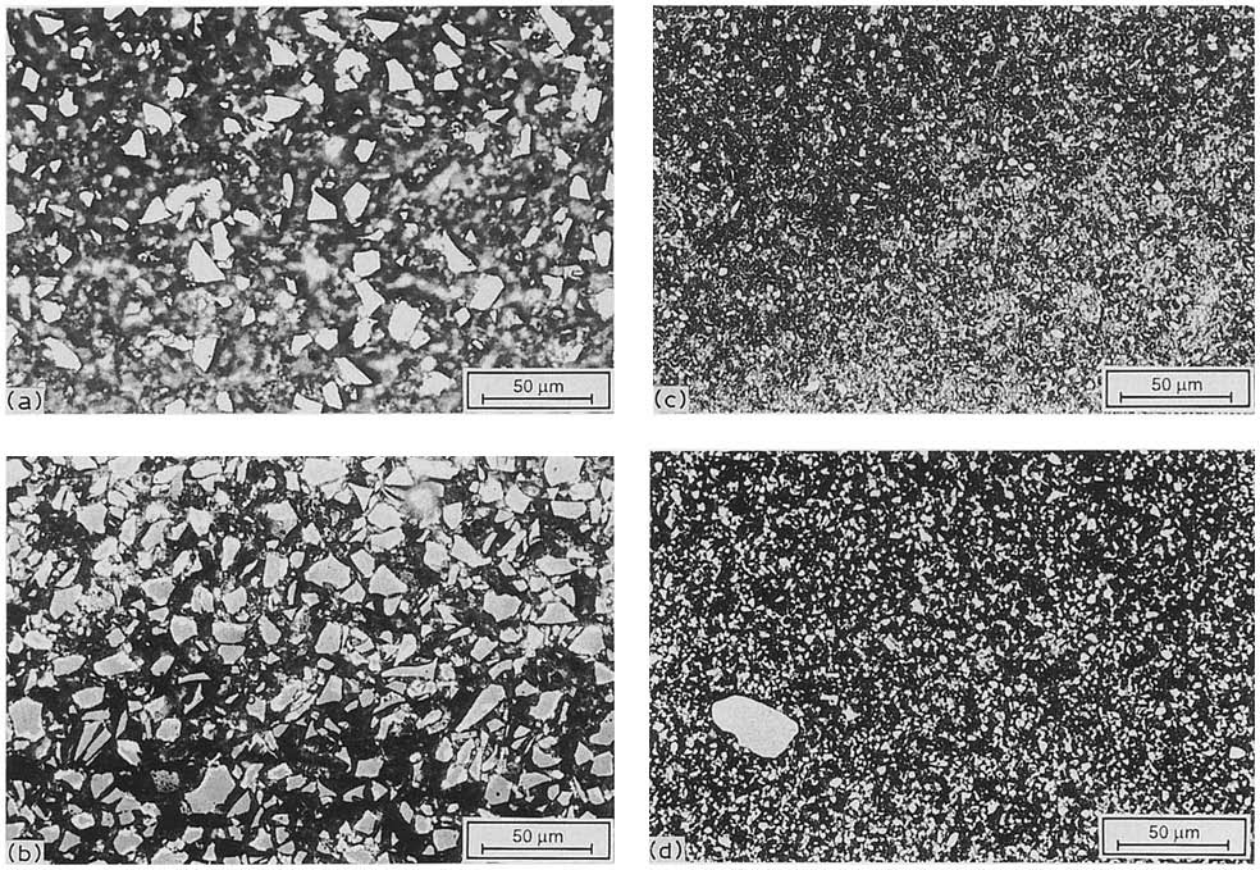

Figure 1 Polished cross-sections of dental composites containing different amounts of particles (V_f) with different sizes (d): (a) $d = 10$ μm, $V_f = 30\%$ nominal; (b) $d = 10$ μm, $V_f = 60\%$ nominal; (c) $d = 2$ μm, $V_f = 20\%$ nominal; (d) $d = 2$ μm, $V_f = 50\%$ nominal.

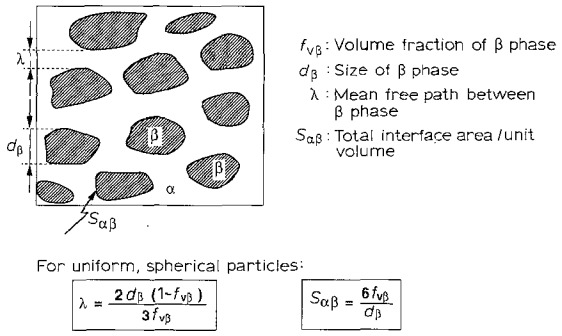

Figure 2 Microstructural parameters in a two-phase isotropic material [5, 6].

TABLE II Relationship between particle distance λ and filler diameter as a function of filler volume fraction, according to the equation $\lambda = 2d(1 - V_f)/3V_f$

Filler vol. fraction V_f(%)	Particle distance λ (μm) $d = 2$ μm	$d = 10$ μm
5	25.30	126.50
10	11.97	59.90
15	7.54	37.74
20	5.32	26.64
25	3.99	20.00
30	3.10	15.50
35	2.47	12.40
40	2.00	9.99
45	1.63	8.14
50	1.33	6.66
55	1.06	5.45
60	0.89	4.44

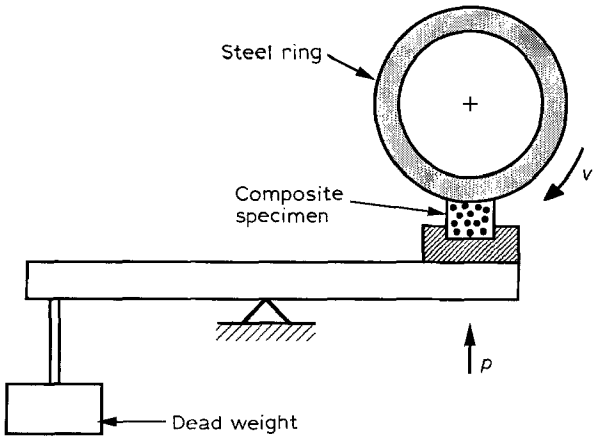

Figure 3 Schematic of a block-on-ring-test configuration.

filler particles are presented in Fig. 1 [5, 6]. These micrographs allow a comparison of the actual distances between the particles and the mean free paths between them, as calculated according to the equation for λ given in Fig. 2. The calculated values are listed in Table II, and they are in a reasonably good agreement with the average distances estimated from the polished cross-sections.

3. Specific wear rates and sliding wear mechanisms

The sliding wear experiments with these dental composites were performed under block on ring configuration against 100 Cr 6-steel with surface roughness values of $R_a = 1.6$ μm and $R_z = 7$ μm (Fig. 3). As the composites were rather brittle (about $K_c = 2.5$ MPa $m^{1/2}$), the loading conditions were chosen so that fracture of wear specimens under applied pressure and surface shear due to the sliding counterpart could be prevented ($p = 0.1$ MPa, $v = 4$ m s^{-1}). Fig. 4 illustrates the course of the specific wear rates of all the materials listed in Table I as a function of filler volume fraction. Both, the 2 μm and 10 μm particle-filled composites show, relative to the unfilled matrix, a little reduction in wear rate at low filler content (up to 10 vol%). Above this value, the composites' wear rates exceed that of the PMMA matrix and run through a maximum, which is much higher and steeper for the 2 μm particulate composite than for the 10 μm system. After these maxima (which are at about $V_f = 20\%$ for the 10 μm and about 28% for the 2 μm composite) the values of both multiphase materials approach each other at a level comparable to that of the neat polymer (in the range above $V_f > 45\%$). Regarding the surface treatment of the fillers and the addition of an antioxidant, there was no systematic effect detectable in the case of the 2 μm-particle system. In the maximum region of the 10 μm composite, the silane treated materials resulted in slightly better values of wear resistance.

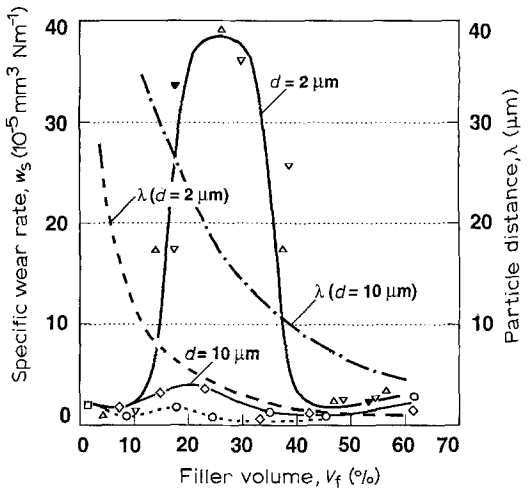

Figure 4 Specific wear rates of dental composites as a function of actual particle content. In addition the course of the particle distances λ (V_f) in the different systems is illustrated.

An analysis of the worn surfaces, as performed by light optical and scanning electron microscopy (SEM), gives an idea of the types of mechanisms involved in material removal. Fig. 5 illustrates for the 2 μm system that the macroscopic appearance of the worn surfaces is dominated by a striation pattern (with their orientation parallel to the sliding direction). This pattern is clearly visible up to a filler content of about 40% (Fig. 5a and b). Above this range the striations are superimposed by a patchwork pattern consisting of regions (Fig. 5c) which increase in number and become larger with further increase in filler content. The same features appeared also on the worn surfaces of the 10 μm system, except that the transition from striations to patches occurred at between 30 and 40% (nominal) for the non-silane treated and between 20

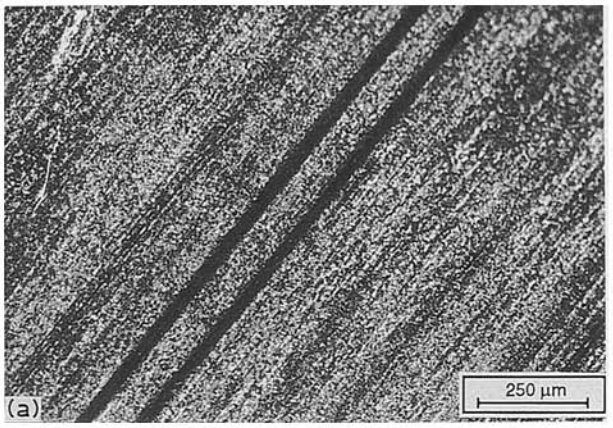

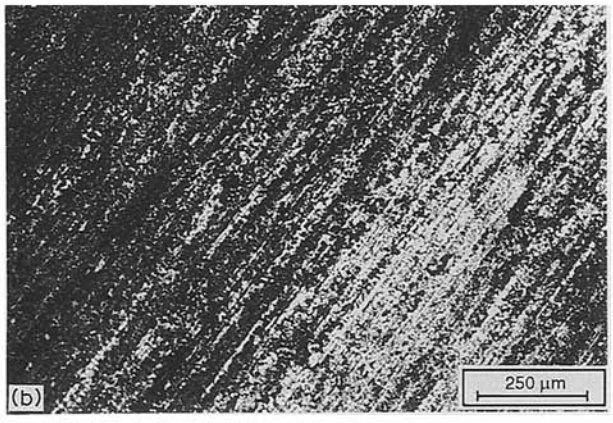

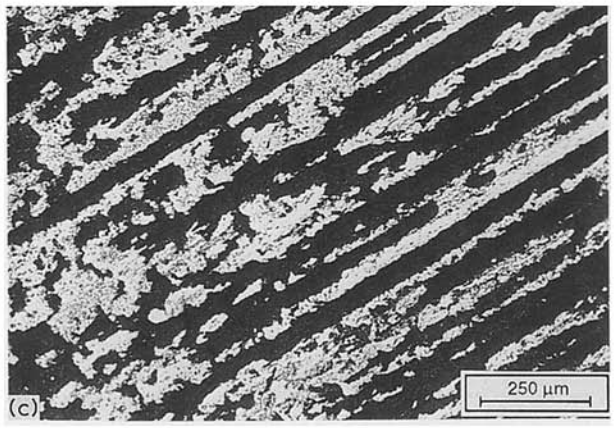

Figure 5 Reflected light micrographs of the worn surfaces of the 2 µm composites demonstrate the transition from striation patterns (a) for $V_f = 20\%$ nominal and (b) for $V_f = 40\%$ nominal to a striation/patchwork pattern (c) $V_f = 55\%$ nominal.

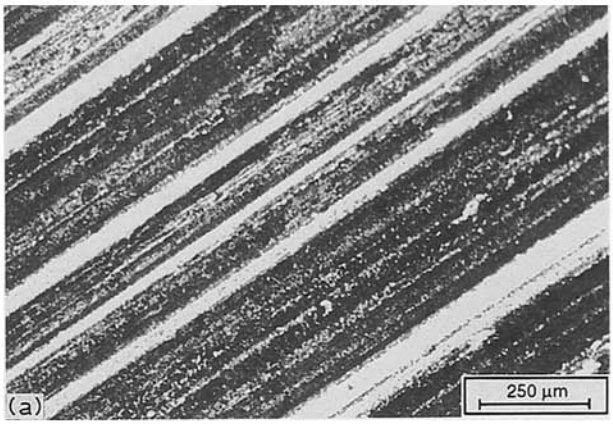

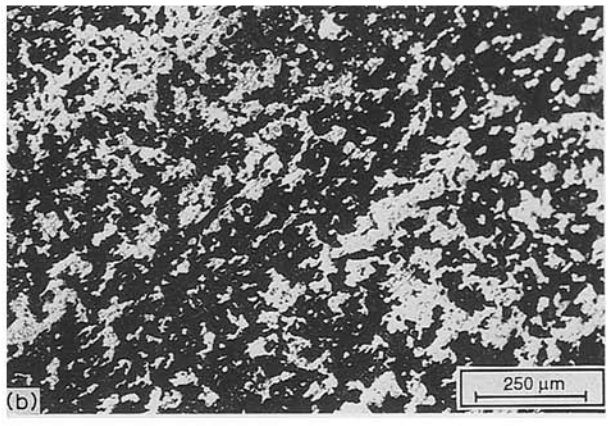

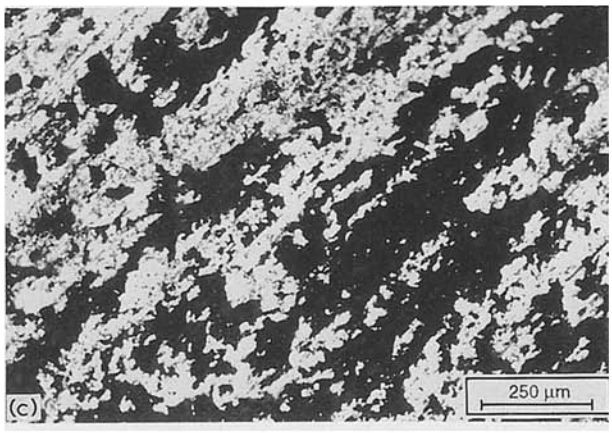

Figure 6 Striations (a) on the worn surface of a 10 µm silane treated composite at $V_f = 10\%$ (nominal) change to a pronounced patchwork pattern (b) at $V_f = 40\%$ (nominal). (c) The size of patches increases with further filler content (e.g. $V_f = 50\%$).

and 30% for the silane treated composite (Fig. 6a to c). Higher magnifications of the different features by the use of SEM showed, that the striation pattern consists of very smooth regions and others having a rough structure with longitudinal and transverse cracks at their edges to the smooth striation (Fig. 7a and b). The latter also appear to be slightly higher in elevation that the rougher, severely worn tracks.

An analogy to this observation was found in case of the patchwork pattern (Fig. 7c and d). The patches consisted of flat, smooth regions, between which a fine grain structure of worn material was found. The more of these patches that are formed and the better they become connected to each other, the more this grainy material remains attached to the wear surface between these patches. The patches themselves seem to consist of back-transferred wear debris which has become entrapped by the worn surface underneath and which, in this way, temporarily protects the latter. The fine cracks in these smooth layers indicate that part of the material will, after some time, separate again from these patches, become new wear debris, and eventually become back-transferred at another location. In the case of the striations, which run from one end of the sample to the other, wear debris formed in the rougher regions gets almost totally removed from the surface at the end of the sample. Only at the edges to the smooth striations can some of it be temporarily collected, before it is cracked and delaminated again. This leads therefore to higher wear of material than in the

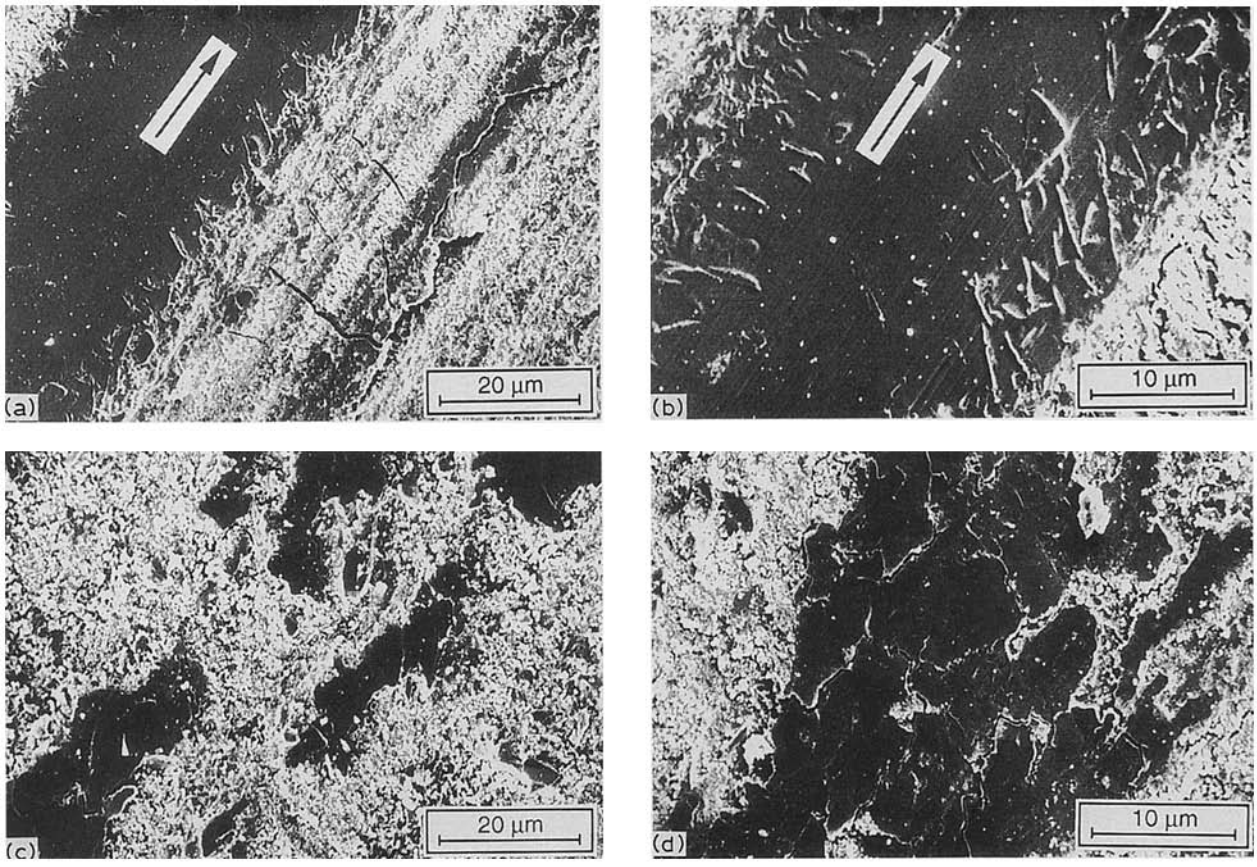

Figure 7 SEM-micrographs of the worn surfaces of a dental composite at $V_f = 10\%$ with rough (right) and smooth (left) striations (a and b; arrow indicates sliding direction). In comparison, the patchwork pattern of smooth patches (looking dark) with grainy areas around (as occurs at higher values of V_f) is shown at (c) and (d).

case where a dense patchwork pattern has built up on the material to be worn.

4. Model description of wear

The rather complex shapes of the wear curves are a result of various mechanisms which dominate the materials wear behaviour in the different ranges of filler volume fraction. The contribution of the individual mechanisms to the total wear of the composites is further controlled by the size of the filler particles and their adhesion to the polymer matrix. In the case of the 2 µm system, the composite seems to follow, in the range up to $V_f = 10\%$, an inverse rule of mixture (IROM), i.e. it is dominated by the simultaneous wear of the matrix with some improvement due to the harder, more wear resistant filler particles. As their distance λ is much greater than the maximum roughness value R_z, there is no particle–particle interaction. The wear surface comprises mainly smooth striations as shown in Fig. 7a. When V_f becomes greater than 10%, λ is equal to or up to 15% smaller than R_z. At this point, a strong interaction between the roughness profile of the steel counterpart and the densely packed, fine particles ($d < R_z$) takes place. Plowing of particles out of the surface starts to dominate the wear process, and these particles can then act as third-body abrasives to the material itself. Once this mechanism is locally initiated it quickly leads to the formation of the rough striations. The probability of this effect is enhanced the more particles there are in the system. In addition, cracks formed at sharp edges of the particles can easily grow under vibrational motion of the rotating steel ring. They can connect with each other due to the shorter particle distances, thus leading to surface fatigue effects and disconnection (in the form of larger patches) from the surface and transport out of the striation at the end of the contact surface, i.e. enhanced wear of the composite. Near a V_f value of 25% however, a counter-mechanism starts to build up, which can be termed 'patching' or 'back-transfer' of worn material [7]. This is now possible because the particle distances approach the particle diameter ($2d > \lambda > d$) which makes it more difficult for the counterpart asperities (roughness profile) to penetrate into the surface and to initiate the plowing mechanism. This results in the worn matrix material, temporarily removed from the spaces between the particles, becoming entrapped between the harder particles having their tips protruding from the surface. At this point, the macroscopic appearance of the wear surface tends to change from a striation to a patchwork pattern. As the patches on the one hand protect the underlaying composite material from momentary wear, and at the same time create a free distance between the steel surface and the areas not covered with patches of back-transferred material, wear is drastically lower than in V_f cases where the plowing mechanism dominates the process. Above $V_f = 45\%$ an equilibrium situation is reached which consists of (a) simultaneous filler and matrix wear, (b) some loosening of particles due to surface fatigue, thus a small

contribution of third-body abrasion, and (c) the formation of patches on the surface for temporary wear protection. The result in this case is a wear rate level similar to that of the neat matrix.

In case of the 10 μm system, the same statements as made for the 2 μm system are valid for the region of lower filler content ($V_f = 10\%$). Above this level ($10\% < V_f < 20\%$), there will be only occasional pulling out of particles (mainly because $d > R_z$ and $\lambda > R_z$); this can, however, also create the formation of striations which are rougher in nature than the smooth parts where the IROM is applicable. The increase of wear by this effect is very much lower than that seen for the 2 μm particles. In contrast to the statement made by other authors [6], it is of particular importance that, under this condition (i.e. where the size of the microstructural details (λ, d) is greater than the asperity size (R_z), the bonding between the components is well organized. Under strong filler/matrix bonding, pull out of harder particles by the roughness tips of the steel counterpart is much more difficult, and therefore the formation of third-body abrasives is reduced (Fig. 8a). This is the reason why the silane treatment in this part of the 10 μm curve showed a clear effect. On the other hand it can be expected that better bond quality is rather ineffective when the asperity size is much greater than the particles and when there is enough space between them that the asperities can locally penetrate into the matrix deep enough to dig out the full particle with matrix around it (Fig. 8b).

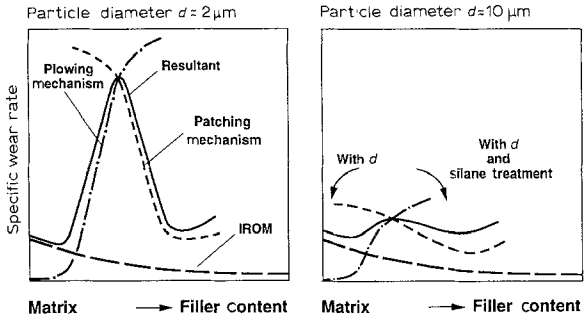

Figure 9 Schematic illustration of the various trends due to the different wear mechanisms and the actual courses of curves resulting from them.

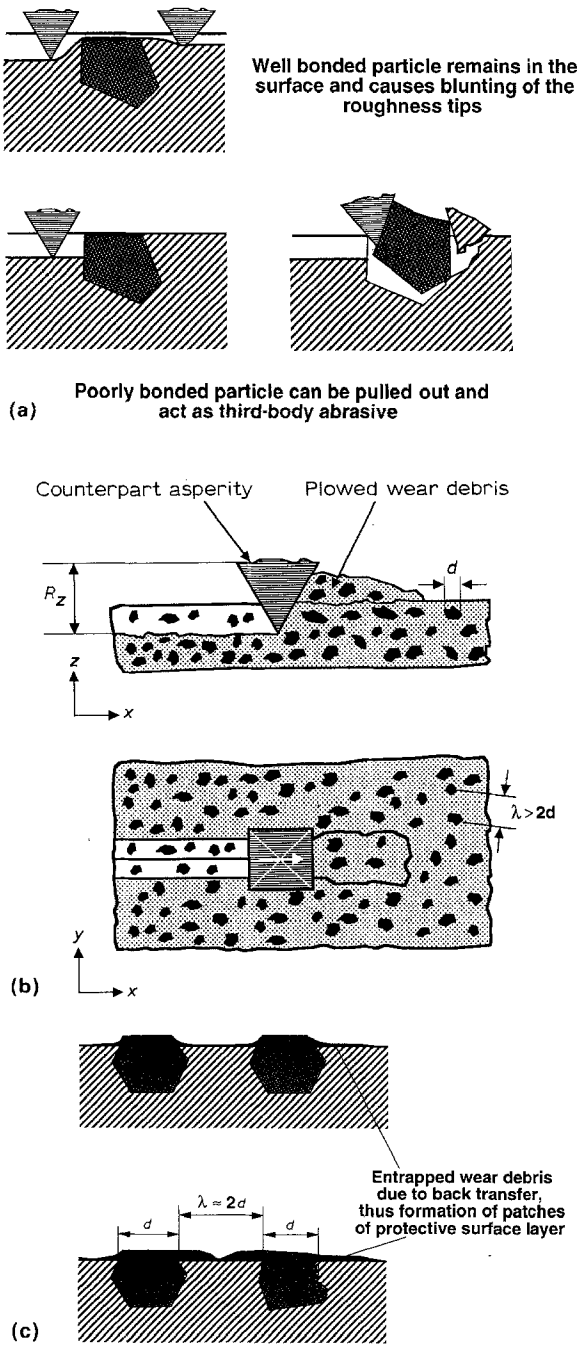

Figure 8 Schematic illustration of the individual wear mechanisms as a function of filler size, bond quality and particle content: (a) effect of silane treatment on the interaction between counterpart asperities and large (10 μm) particles ($d > R_z$; $\lambda > R_z$); (b) plowing of fine (2 μm) particles out of the surface ($d < R_z$; $\lambda > 2d$); (c) formation of a protective layer between embedded hard particles of short distance ($2d \geq \lambda > d$)

Due to the greater particles size and the fact that most of them remain in the wear surface, the plowing mechanism in the 10 μm system is replaced earlier by the patching mechanism. Hard particles, which stick out of the worn PMMA matrix easily begin to capture worn material at their edges, thus forming a patchwork pattern under the condition that λ approaches the particle size ($2d \geq \lambda > d$) (Fig. 8c). The optimum protection is reached when $\lambda \approx d$. This is again combined with a reduction in wear rate until an equilibrium level is reached which is slightly lower than that seen for the 2 μm material.

In summary, the different trends in specific wear rate versus filler volume fraction due to the action of various mechanisms are schematically illustrated in Fig. 9, along with the actual curves resulting from them. The complexity does not allow description of these curves by a simple rule of mixtures; the only attempt which can be made to approach these trends mathematically is a semi-empirical relationship which includes (besides the rule of mixture components) special terms which account for the individual mechanisms dominating the composite wear process in the various regions of V_f. A simpler development of such an equation has been performed by Friedrich and Voss [8, 9] for sliding wear of short fibre composites. Further time and experiments are, however, needed to verify how this approach must be modified in order to be useful for a full description of the results presented in this paper.

Acknowledgements

The author acknowledges the help and cooperation of Dr O. Jacobs and Mr D. Sülthaus during the experimental testing procedure. Further thanks are due to Dr T.A. Roberts, ICI Chemicals and Polymers, for preparation and delivery of the testing materials. The support of the Fond Der Chemischen Industrie, Frankfurt, for the authors personal research activities in 1993 is also gratefully acknowledged.

References

1. S. V. PRASAD and P. D. CALVERT, *J. Mater. Sci.* **15** (1980) 1746.
2. D. C. WATTS, in "Materials Science and Technology, Vol. 14: Medical and Dental Materials" (Vol. ed. D. F. Williams) (VCH-Publishers, New York, 1992) p. 109.
3. A. J. DE GEE, P. PALLAV and C. L. DAVIDSON, *J. Dent. Res.* **65** (1986) 654.
4. T. A. ROBERTS, ICI Chemicals & Polymers, private communication, October 1990.
5. K. FRIEDRICH, "Advances in composites tribology", edited by K. Friedrich (Elsevier Science Publishers, Amsterdam, 1993) to be published.
6. W. SIMM and S. FRETI, *Wear* **129** (1989) 105.
7. M. GODET, *ibid.* **100** (1984) 437.
8. K. FRIEDRICH, in "Friction and wear of polymer composites", edited by K. Friedrich (Elsevier Science Publishers, Amsterdam, 1986) p. 233.
9. H. VOSS, "Aufbau, Bruchverhalten und Verschleißeigenschaften kurzfaserverstärkter Hochleistungsthermoplaste", Fortsch.-Ber. VDI-Zeitschr. Reihe 5, Nr. 116, VDI-Verlag, Düsseldorf (1987).

Received 14 October
and accepted 19 November 1992